View Article Online
View Journal

Materials
Advances

This article can be cited before page numbers have been issued, to do this please use: W. Takeda and P. Lucas, *Mater. Adv.*, 2026, DOI: 10.1039/D6MA00442C.

View Article Online
DOI: 10.1039/D6MA00442C

Relationship between Enthalpy Fluctuation and Nonexponential Relaxation in Glass-forming Liquids

Wataru Takeda and Pierre Lucas

Department of Materials Science and Engineering, University of Arizona, Tucson, AZ 85712, United States

Abstract:

A relationship between the equilibrium fictive temperature fluctuation $\sigma_{T_\mathrm{f}^\mathrm{e}}$ and the nonexponentiality β_KWW is derived by extending the Adam-Gibbs equation within Donth's fluctuation-dissipation theorem to introduce a quantitative account for dynamic heterogeneity of supercooled liquids. The framework is validated against three structurally, chemically, and kinetically distinct glass-forming systems, namely $\mathrm{B_2O_3}$, $\mathrm{Pd_{43}Cu_{27}Ni_{10}P_{20}}$, and PVAc, without any adjustable fitting parameters. A condition for time-temperature superposition (TTS) is further derived as a balance between the fictive temperature fluctuation rate and a configurational term composed of the configurational entropy and heat capacity difference between glass and liquid. The present framework reveals the interplay between thermodynamic quantities, enthalpy fluctuations, and dynamic heterogeneity in glass-forming liquids.

I. Introduction

Dynamic heterogeneity is a fundamental characteristic of glass-forming liquids [1,2]. As they approach the glass transition, distinct spatial regions relax at different rates, giving rise to a broad spectrum of relaxation times and the characteristic nonexponential relaxation response [3]. This nonexponential behavior is commonly described by the Kohlrausch–Williams–Watts (KWW) function [4,5], whose stretching exponent β_KWW reflects the width of the underlying distribution of relaxation times, where $\beta_\mathrm{KWW} = 1$ corresponds to Debye relaxation and decreasing values of β_KWW corresponds to increasingly broader spectrum of relaxation times. Each spatial region may relax exponentially or may have an intrinsic nonexponentiality β_0 [6]. The global relaxation is then understood to be a superposition of local relaxation processes weighted by a distribution of relaxation times $X(\ln\tau)$:

$$\int_{-\infty}^{\infty} X(\ln\tau)\exp\left[-\left(\frac{t}{\tau}\right)^{\beta_0}\right]d\ln\tau = \exp\left[-\left(\frac{t}{\tau_\mathrm{KWW}}\right)^{\beta_\mathrm{KWW}}\right], (1)$$

where the right-hand side is the KWW function and β_KWW is the macroscopic stretching exponent, and τ_KWW is related to the average relaxation time as $\langle\tau\rangle = \tau_\mathrm{KWW}\Gamma(\beta_\mathrm{KWW}^{-1}+1)$, where Γ is the gamma function. Eq.1 links β_KWW directly to the underlying dynamic heterogeneity: in the homogeneous limit where all subsystems share a single relaxation time, $X(\ln\tau)\rightarrow\delta(\ln\tau-\ln\tau_0)$, where δ denotes Dirac's delta function, the macroscopic exponent reduces to the intrinsic value, $\beta_\mathrm{KWW}\rightarrow\beta_0$. A key observation is that β_KWW is not a material constant but depends on temperature [7–10].

View Article Online
DOI: 10.1039/D6MA00442C

According to Angell, glass-forming liquids can be classified as strong or fragile depending on the temperature dependence of their relaxation time or, equivalently, their viscosity, and can be characterized by the fragility index m, defined as the slope $d\log_{10}\tau/d(T_\mathrm{g}/T)$ evaluated at the glass transition temperature T_g [11]. Fragility has been correlated with several dynamic and thermodynamic properties, including the configurational entropy S_c [12], the heat capacity difference between liquid and glass [13,14], the stretching exponent at T_g $\beta_\mathrm{KWW}(T_\mathrm{g})$ [15], and the temperature dependence of β_KWW [16,17]. When β_KWW remains constant over a range of temperature, the relaxation-time spectrum preserves its shape, a condition known as time–temperature superposition (TTS). Dielectric studies [17,18] and shear mechanical spectroscopy [16] across a wide range of glass-forming liquids have shown a clear trend where more fragile liquids tend to maintain TTS over a broader range of relaxation time. However, no unified thermodynamic framework has been established that quantitatively predicts the conditions under which TTS holds or breaks down.

Understanding the temperature dependence of β_KWW requires examining how relaxation time fluctuations arise from thermodynamic fluctuations. As established by Donth's fluctuation-dissipation theorem (DFDT) [19,20], the distribution of relaxation times maps onto the fictive temperature fluctuation $\sigma_{T_\mathrm{f}^\mathrm{e}}$, which, since the equilibrium fictive temperature is proportional to the enthalpy, is fundamentally rooted in the distribution of local enthalpies [21,22]. A distribution of enthalpy in supercooled liquids has been observed in both experiments and simulations [22–25]. While the connection between enthalpy fluctuations, the distribution of relaxation times, and β_KWW is physically well motivated, a quantitative relationship linking the dynamic heterogeneity characterized by nonexponential relaxation to the fictive temperature fluctuation through rigorously defined thermodynamic quantities, such as the configurational entropy and heat capacity, has not yet been developed.

In this work, we expand on a phenomenological model, the Takeda-Lucas (TL) model [26], to develop a thermodynamic framework that connects the Adam-Gibbs relation [27] to dynamic fluctuations. While the TL model accounts for both equilibrium and nonequilibrium states, the present generalization focuses on the equilibrium supercooled liquid, where the thermodynamic quantities are well defined. This yields a parameter-free prediction connecting $\sigma_{T_\mathrm{f}^\mathrm{e}}$ and β_KWW, through $S_\mathrm{c}(T)$ and $\Delta C_\mathrm{p}(T)$. We validate the framework against three chemically, structurally, and kinetically distinct glass-forming systems: $\mathrm{B_2O_3}$ (network oxide, $m = 36$ [28]), $\mathrm{Pd_{43}Cu_{27}Ni_{10}P_{20}}$ (metallic alloy, $m = 69$ [29]), and PVAc (polymer, $m = 95$ [15]). Furthermore, we derive a condition for TTS in terms of a balance between the fictive temperature fluctuation rate and a configurational term, revealing the interplay between the thermodynamic quantities $S_\mathrm{c}(T)$, $\Delta C_\mathrm{p}(T)$, the enthalpy fluctuation captured by $\sigma_{T_\mathrm{f}^\mathrm{e}}$, and the temperature dependence of nonexponentiality in glass-forming liquids.

The paper is organized as follows. In Sec. II, we briefly review the TL model of dynamic heterogeneity. In Sec. III, we present the heterogeneous extension of Adam-Gibbs (AG) theory with DFDT formalism and derive the key equations. In Sec. IV, we validate the framework against three glass-forming systems. In Sec. V, we verify the predicted condition for TTS, in Sec. VI we discuss the implications of the developed framework, and Sec. VII concludes the paper.

View Article Online
DOI: 10.1039/D6MA00442C

II. TL model of supercooled liquids and glasses

The TL model accounts for both enthalpy fluctuation and temperature-dependent β_{KWW} by introducing a distribution of equilibrium fictive temperatures that maps to a distribution of relaxation times via DFDT [19,26,30,31]. The enthalpy fluctuation is modeled by the fictive temperature fluctuation, using the definition that fictive temperature T_{f} is proportional to enthalpy H, $T_{\mathrm{f}} \propto H$. The model accounts for the heterogeneity of the supercooled liquid by introducing a distribution of equilibrium fictive temperatures $T_{\mathrm{f}}^{\mathrm{e}}$ and for the temperature dependence of nonexponentiality by introducing a temperature dependent distribution of relaxation time. This is achieved using Cangialosi *et al.*'s formulation of dynamic heterogeneity which relates the distribution X of relaxation times to a distribution Y of Vogel temperatures [32] and further relating it to a distribution W^{e} of equilibrium fictive temperatures $T_{\mathrm{f}}^{\mathrm{e}}$ as:

$$X d\ln\tau = Y dT_{\mathrm{v}} = W^{\mathrm{e}} dT_{\mathrm{f}}^{\mathrm{e}}, \quad (2)$$

The detailed equations of the TL model (discretized domain weights, relaxation time expressions, and skewness parameters) are provided in Ref. [26]. The key result relevant to the present work is the connection between the fluctuation of fictive temperatures, i. e. the width of the distribution or the variance of fictive temperatures and the fluctuation of relaxation times through DFDT formalism [19,26,30,31]:

$$\delta T = \sigma_{T_{\mathrm{f}}^{\mathrm{e}}} = \frac{\sigma_{\ln\tau}}{\left|\frac{\partial\langle \ln\tau(T)\rangle}{\partial T}\right|}, (3)$$

where $\sigma_{T_{\mathrm{f}}^{\mathrm{e}}}$ is the fluctuation (variance) of equilibrium fictive temperatures and $\sigma_{\ln\tau}$ is the fluctuation of the relaxation time in equilibrium (see the detailed derivation of Eq.3 in the supplementary material SM). Furthermore, the relaxation time for each domain i of the distribution is determined by the local Vogel temperature $T_{\mathrm{v},i}$ using the Adam-Gibbs equation modified by Hodge (AGH) [33,34] as

$$\tau_i = \tau_0 \exp\left(\frac{D T_{\mathrm{v},i}}{T\left(1 - \frac{T_{\mathrm{v},i}}{\langle T_{\mathrm{f}}\rangle}\right)}\right), (4)$$

In equilibrium, $\langle T_{\mathrm{f}}\rangle = T$, and Eq. 4 adopts the Vogel–Fulcher–Tammann (VFT) form:

$$\tau_i = \tau_0 \exp\left(\frac{D T_{\mathrm{v},i}}{T - T_{\mathrm{v},i}}\right), (5)$$

where D is the strength parameter related to the fragility index m [15]. $T_{\mathrm{v},i}$ determines the amplitude of the activation energy for each domain and its distribution is temperature independent (Fig. 1(a)). Finally, an expression for the equilibrium fictive temperature of ith domain $T_{\mathrm{f},i}^{\mathrm{e}}$ that satisfies both DFDT and the VFT equation in Eq. 5, is given by [26]:

$$T_{\mathrm{f},i}^{\mathrm{e}} = T\left(2 - \frac{T_{\mathrm{v},i}}{\langle T_{\mathrm{v}}\rangle}\right). \quad (6)$$

Eq. 6 effectively makes the distribution of $T_{\mathrm{f}}^{\mathrm{e}}$ temperature dependent.

View Article Online
DOI: 10.1039/D6MA00442C

Indeed, it is important to recall that the distribution of local fictive temperatures is determined by both the weights W_i^{e} and the positions $T_{\mathrm{f},i}^{\mathrm{e}}$. In our framework the weights W_i^{e} are temperature-independent, so the temperature dependence of the distribution width enters entirely through the positions $T_{\mathrm{f},i}^{\mathrm{e}}$, which evolve with temperature at rates defined by their respective $T_{\mathrm{v},i}$ per Eq. 6. Hence, the width of the distribution is temperature-dependent (Fig. 1(b)). This accounts for the temperature dependence of the distribution of enthalpy fluctuations.

Finally, a discretized distribution of weight X_i for τ_i is obtained from the weights Y_i of the Vogel temperatures $T_{\mathrm{v},i}$ according to:

$$X_i = Y_i \frac{T}{D}\left(1 - \frac{T_{\mathrm{v},i}}{T_{\mathrm{f}}}\right)^2. \quad (7)$$

Consequently, per Eq. 6&7, both the shape and the width of the distribution of relaxation times are temperature dependent, which accounts for the temperature dependence of nonexponentiality (Fig. 1(c)).

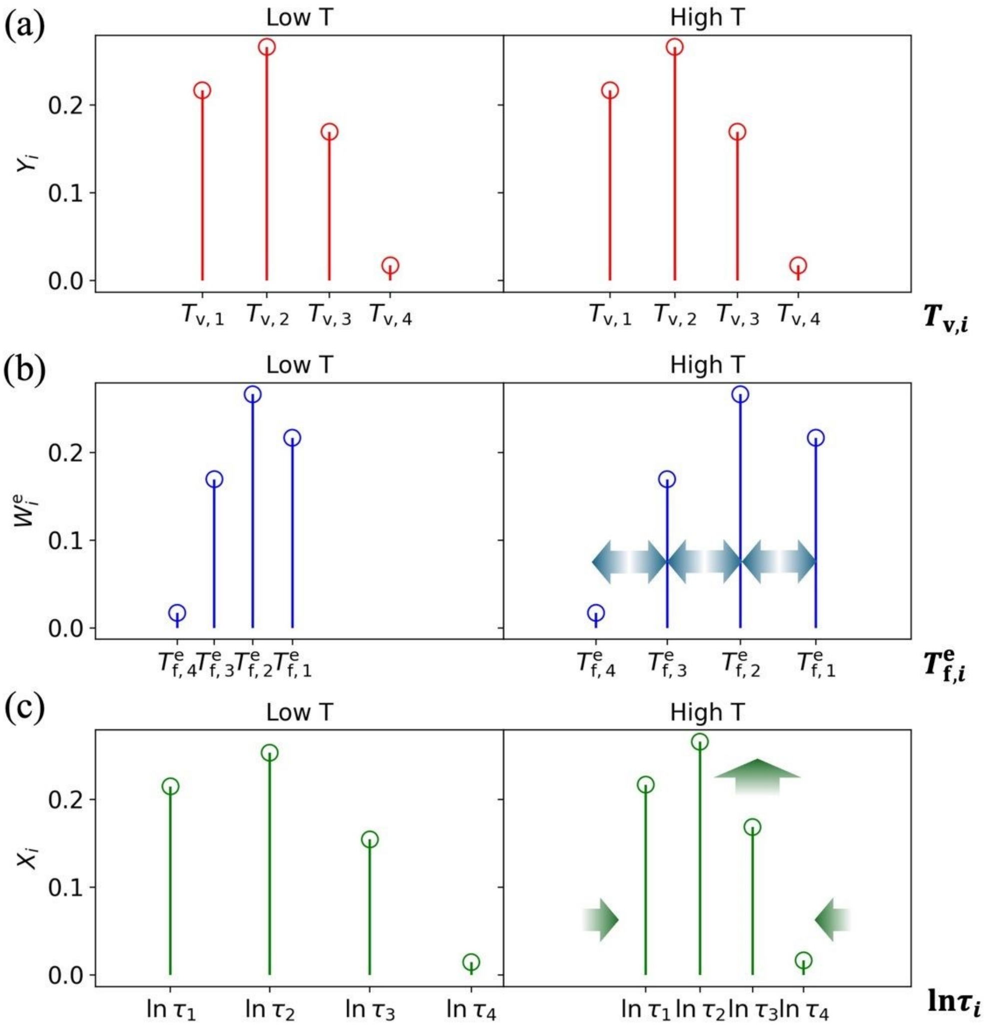

FIG 1. Schematics of the temperature dependence of the discrete distribution for (a) the Vogel temperatures, (b) the equilibrium fictive temperatures, (c) the relaxation time.

View Article Online
DOI: 10.1039/D6MA00442C

III. Heterogeneous Adam-Gibbs Theory applied to the TL model

The TL model is based on the AGH equation in Eq. 4. This form of AG equation approximates the configurational entropy S_c by assuming the temperature dependence of the difference in heat capacity between the glass C_p^g and the liquid C_p^l to be inversely proportional to temperature as:

$$\Delta C_\mathrm{p}(T) = \frac{C}{T},(8)$$

where ΔC_p is the heat capacity difference defined as $C_\mathrm{p}^\mathrm{l} - C_\mathrm{p}^\mathrm{g}$, and C is the proportionality constant, where this form was conveniently chosen so that when $T_\mathrm{f} = T$, Eq. 4 goes back to the ordinary VFT equation in Eq. 5. Thus, the formulated heterogeneous model above is limited to a system in which Eq. 8 holds. Here we generalize the TL–DFDT formalism to arbitrary temperature dependences of $\Delta C_\mathrm{p}(T)$ commencing from the original Adam–Gibbs equation [27,35]. While doing so, we establish a connection between the nonexponentiality β_KWW, the enthalpy fluctuation $\sigma_{T_\mathrm{f}^\mathrm{e}}$, the configurational entropy S_c, and ΔC_p.

Let us begin by restating the original AG equation as

$$\tau = \tau_0 \exp\left(\frac{A}{TS_\mathrm{c}(T)}\right),(9)$$

where A is the energy barrier for cooperative rearrangement. We assume that the heterogeneity in relaxation time comes entirely from the heterogeneity in the energy barrier A following the treatment by Gupta and Mauro in Ref.[35]. We further assume that the effect of heterogeneity can be captured by a number of discrete sets of domains N where the relaxation time of ith domain based on Eq. 9 becomes

$$\tau_i = \tau_0 \exp\left(\frac{A_i}{TS_\mathrm{c}(T)}\right),(10)$$

where A_i is the activation energy for domain i. We treat the configurational entropy as a bulk property that remaining uniform across all domains, while A_i captures the local dynamic variation. Thus, the average relaxation time becomes

$$\langle\tau\rangle = \tau_0 \exp\left(\frac{\langle A\rangle}{TS_\mathrm{c}(T)}\right),(11)$$

where the angle brackets denote averaged quantities.

A. Enthalpy fluctuation and nonexponentiality

The DFDT framework establishes that fluctuations in relaxation time map to fluctuations in fictive temperature through Eq. 3.

From Eq. 11, the denominator in Eq. 3 becomes

$$\frac{\partial\langle \ln\tau(T)\rangle}{\partial T} = \langle A\rangle\left(-\frac{1}{T^2 S_\mathrm{c}(T)} - \frac{1}{TS_\mathrm{c}(T)^2}\frac{dS_\mathrm{c}(T)}{dT}\right) = -\frac{\langle A\rangle}{T^2 S_\mathrm{c}(T)}\left[1 + \frac{\Delta C_\mathrm{p}(T)}{S_\mathrm{c}(T)}\right],(12)$$

where we use the identity $dS_\mathrm{c}/dT = \Delta C_\mathrm{p}(T)/T$.

View Article Online
DOI: 10.1039/D6MA00442C

Thus, by inserting Eq. 12 into Eq. 3, $\sigma_{\ln\tau}$ can be expressed in terms of $\sigma_{T_\mathrm{f}^\mathrm{e}}$ as

$$\sigma_{\ln\tau} = \frac{\sigma_{T_\mathrm{f}^\mathrm{e}}\langle A\rangle}{T^2 S_\mathrm{c}(T)}\left[1+\frac{\Delta C_\mathrm{p}(T)}{S_\mathrm{c}(T)}\right].\ (13)$$

Richert and Richert show that the fluctuation (variance) of relaxation time can be expressed in terms of nonexponential parameter β_KWW and intrinsic nonexponentiality β_0 as [36]:

$$\sigma_{\ln\tau}^2 = \frac{\pi^2}{6}\left(\frac{1}{\beta_\mathrm{KWW}^2}-\frac{1}{\beta_0^2}\right).\ (14)$$

We can then obtain an expression for β_KWW by inserting Eq. 13 into Eq. 14, and solving for β_KWW gives:

$$\beta_\mathrm{KWW}(T) = \frac{1}{\sqrt{\beta_0^{-2}+\mathit{\Lambda}(T)^2}},(15)$$

where $\mathit{\Lambda}(T)$ is defined as

$$\mathit{\Lambda}(T) = \frac{\sqrt{6}}{\pi}\frac{\langle A\rangle}{S_\mathrm{c}(T)}\frac{\sigma_{T_\mathrm{f}^\mathrm{e}}(T)}{T^2}\left[1+\frac{\Delta C_\mathrm{p}(T)}{S_\mathrm{c}(T)}\right].\ (16)$$

Thus, Eq. 15 relates the dynamic heterogeneity β_KWW, the fictive temperature fluctuation $\sigma_{T_\mathrm{f}^\mathrm{e}}$, and the configurational entropy $S_\mathrm{c}(T)$, all of which are experimentally accessible. In most cases, the absolute value of S_c is not experimentally available, thus, one may use the approximation $S_\mathrm{c} \approx S_\mathrm{ex}$, where S_ex is the excess entropy obtained by integrating the $\Delta C_\mathrm{p}(T)/T$.

B. A condition for time-temperature-superposition (TTS)

One of the hallmark questions in glass science is in which systems, and over what temperature ranges, does time–temperature superposition (TTS) apply in glasses and glass-forming liquids. Based on Eq. 15, we can determine the conditions under which β_KWW increases, remains constant, or decreases with increasing temperature by taking the temperature derivative, as follows:

$$\frac{d\beta_\mathrm{KWW}}{dT} = -\frac{\Lambda(T)}{\left(\beta_0^{-2}+\Lambda(T)^2\right)^{\frac{3}{2}}}\frac{d\Lambda}{dT} = -\frac{\Lambda(T)^2}{\left(\beta_0^{-2}+\Lambda(T)^2\right)^{\frac{3}{2}}}\frac{d\ln\Lambda(T)}{dT},(17)$$

if we exclude the limiting case of $\Lambda = 0$. We note that $\Lambda(T)$ cannot be negative by definition. Thus, the condition for TTS can be obtained by setting $d\ln\Lambda(T)/dT = 0$, and solving for the equilibrium fluctuation term in Eq. 16 as:

$$T\frac{d\ln\sigma_{T_\mathrm{f}^\mathrm{e}}(T)}{dT} = 2+\frac{\Delta C_\mathrm{p}(T)}{S_\mathrm{c}(T)} - T\frac{d}{dT}\ln\left(1+\frac{\Delta C_\mathrm{p}(T)}{S_\mathrm{c}(T)}\right),(18)$$

We introduce two dimensionless parameters: the fictive-temperature fluctuation rate $R(T)$, and configurational term $\mathit{\Xi}(T)$, defined as

$$R(T) = T\frac{d\ln\sigma_{T_\mathrm{f}^\mathrm{e}}(T)}{dT},(19)$$

View Article Online
DOI: 10.1039/D6MA00442C

and

$$\Xi(T) = 2 + \frac{\Delta C_{\mathrm{p}}(T)}{S_{\mathrm{c}}(T)} - T\frac{d}{dT}\ln\left(1 + \frac{\Delta C_{\mathrm{p}}(T)}{S_{\mathrm{c}}(T)}\right), (20)$$

where all the variables are *experimentally measurable.* Both R and Ξ are dimensionless ratios. Finally, we get the conditions for the temperature dependence of β_{KWW} as compiled in Table 1.

Table 1. Derived conditions of temperature dependence of β_{KWW}

Condition	Temperature dependence of β_{KWW}
$R(T) < \Xi(T)$	β_{KWW} increases upon heating
$R(T) = \Xi(T)$	β_{KWW} is constant (TTS condition)
$R(T) > \Xi(T)$	β_{KWW} decreases upon heating

IV. Validation

In this section, we validate the derived heterogeneous AG model with DFDT formalism using three systems: B_2O_3, $Pd_{43}Cu_{27}Ni_{10}P_{20}$, and PVAc. We do so by using *experimentally determined values* of β_{KWW}, $\sigma_{T_{\mathrm{f}}^{\mathrm{e}}}$, and S_{c} to confirm the validity of the relation expressed in Eq. 15, and Eq. 16 with *no adjustable fitting parameters*. These systems were chosen based on the availability of accurate experimental heat capacity data, temperature-dependent nonexponentiality values, and equilibrium fictive temperature fluctuations. Additionally, they span a wide range of fragility, specifically 36 [28], 69 [29], and 95 [15], for B_2O_3, $Pd_{43}Cu_{27}Ni_{10}P_{20}$, and PVAc, respectively, and are structurally and chemically distinct.

Table 2. Summary of the model parameters for the three glass-forming systems. Configurational entropy is anchored at T_{m} (fusion) for B_2O_3, at T_{r} for $Pd_{43}Cu_{27}Ni_{10}P_{20}$, and at T_{K} (Kauzmann) for PVAc. T_{r} is the temperature at which viscosity is 1 Pa · s defined by Gallino *et al*. [34] Units: τ_0 in seconds, ΔS_m and $S_{\mathrm{c}}(T_{\mathrm{r}})$ in J $(\mathrm{mol})^{-1}(\mathrm{K})^{-1}$. The numbers in square brackets indicate the corresponding reference.

	B_2O_3	$Pd_{43}Cu_{27}Ni_{10}P_{20}$	PVAc
T_{g} [K]	560 [17]	568 [34]	311 [37]
T_{m} [K]	723 [17]	Not used	Not used
T_{K} [K]	Not used	Not used	267 [37]
T_{r} [K]	Not used	900 [34]	Not used
S_{c} anchor	$\Delta S_{\mathrm{m}} = 30.5$ [38]	$S_{\mathrm{c}}(T_{\mathrm{r}}) = 11.26$ [34]	$S_{\mathrm{c}}(T_{\mathrm{k}}) = 0$
β_0	1.00	0.76 [39]	0.67 [37]

View Article Online
DOI: 10.1039/D6MA00442C

m_0	16 [15]	Not used	Not used
$\log_{10}\tau_0$	Not used	Not used	−12.08 [37]
$\langle A\rangle$	448,023	114,870 [34]	88,332

In all the analysis below, we first need to obtain $\Delta C_\mathrm{p}(T)$ and $S_\mathrm{ex}(T)$ to compute $S_\mathrm{c}(T)$.

To estimate configurational entropy for $\mathrm{B_2O_3}$, we calculate the excess entropy as

$$S_\mathrm{c}(T) \approx S_\mathrm{ex}(T) = \Delta S_m - \int_T^{T_\mathrm{m}} \frac{\Delta C_\mathrm{p}(T')}{T'} dT', (21)$$

where ΔS_m is the entropy of fusion and $\Delta C_\mathrm{p}(T)$ is the heat capacity difference between liquid C_p^l and glass C_p^g, assuming that the vibrational contribution to the heat capacity in the liquid is the same as that of glassy $\mathrm{B_2O_3}$.

For $\mathrm{Pd_{43}Cu_{27}Ni_{10}P_{20}}$, we follow the procedure of Gallino *et al.* [40] using the temperature at which the viscosity is 1 Pa·s as the reference. Details of these calculations are provided in the SM. For PVAc, where no melting temperature exists, the configurational entropy is obtained by integrating the heat capacity difference from the Kauzmann temperature T_K, estimated by the Vogel temperature. Thus, we assume that $\Delta C_\mathrm{p}(T)$ in three glass-forming systems are purely configurational in origin in all analysis [41].

The heat capacity data for $\mathrm{B_2O_3}$, $\mathrm{Pd_{43}Cu_{27}Ni_{10}P_{20}}$, and PVAc are taken from Ref. [42], Ref. [43], and Ref. [44], respectively. The heat capacity of crystalline $\mathrm{Pd_{43}Cu_{27}Ni_{10}P_{20}}$ was used for the heat capacity of solid following the procedure of Gallino *et al.* [34]

The other necessary parameters for determining $S_\mathrm{c}(T)$ for each system are ΔS_m for $\mathrm{B_2O_3}$, S_c (T_r) for $\mathrm{Pd_{43}Cu_{27}Ni_{10}P_{20}}$, and T_k for PVAc, and the values and corresponding references are compiled in Table 2. Fig. 2 shows the heat capacity data and corresponding fits for $\mathrm{B_2O_3}$ as an example. The heat capacity data and their fits for $\mathrm{Pd_{43}Cu_{27}Ni_{10}P_{20}}$ and PVAc as well as the detail of fitting procedures are shown in the SM.

The calculated S_c and the ratio $\Delta C_\mathrm{p}/S_\mathrm{c}$ as a function of the reduced temperature T/T_g for the three glass-forming systems are shown in Figs. 3(a) and 3(b).

Next, $\langle A\rangle$ and β_0 must be determined to establish the correlation between β_KWW and $\sigma_{T_\mathrm{f}^\mathrm{e}}$ using Eqs. 15&16.

First, $\langle A\rangle$ is derived based on the AG equation in Eq. 11 as

$$\langle A\rangle = \ln\left(\frac{\tau(T_\mathrm{g})}{\tau_0}\right) T_\mathrm{g} S_\mathrm{c}(T_\mathrm{g}) = T_\mathrm{g} S_\mathrm{c}(T_\mathrm{g}) m_0 \ln 10\,. \ (22)$$

$\langle A\rangle$ is determined from Eq. 22 with $m_0 = 16$ for $\mathrm{B_2O_3}$ and with τ_0 obtained by dielectric spectroscopy for PVAc. The experimentally determined $\langle A\rangle$ from viscosity [34] is used for $\mathrm{Pd_{43}Cu_{27}Ni_{10}P_{20}}$. Second, β_0 is set as 1 for $\mathrm{B_2O_3}$, 0.76 for $\mathrm{Pd_{43}Cu_{27}Ni_{10}P_{20}}$ taken from Ref.

View Article Online
DOI: 10.1039/D6MA00442C

[39], and 0.67 for PVAc taken from Ref. [37]. The resulting parameters are summarized in Table 2.

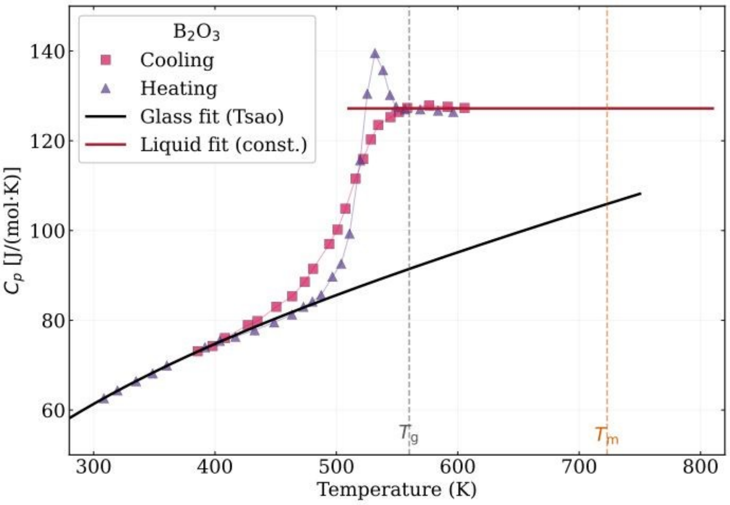

FIG 2. Heat capacities of B_2O_3. The data are taken from Ref. [42]. Cooling and heating in the legend indicates that the data were collected during constant cooling and heating. The semiempirical equation for heat capacity of solid introduced by Tsao *et al.* [45] was used for C_p^g, and the C_p^l was assumed to be constant. The details of the fitting are given in the SM.

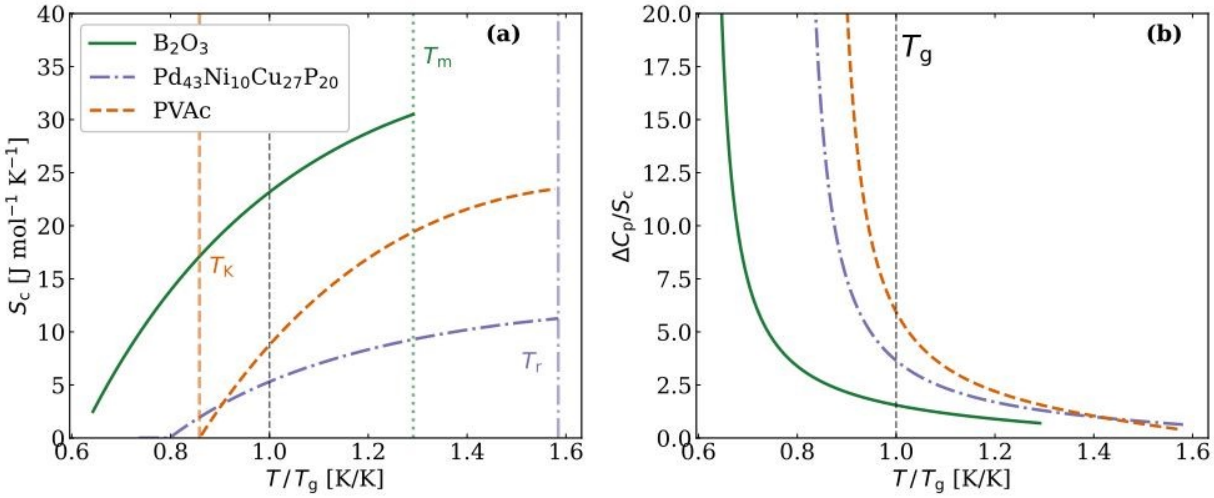

FIG 3. Configurational entropy S_c in (a) and the ratio $\Delta C_p/S_c$ in (b) as a function of the reduced temperature T/T_g for the three glass-forming systems. The black vertical dashed line marks $T/T_g = 1$. The characteristic reference temperatures used to anchor S_c for each system are indicated by vertical lines whose color and style match the corresponding curve: T_m for B_2O_3; T_r for $Pd_{43}Cu_{27}Ni_{10}P_{20}$; T_k for PVAc.

Using the experimentally determined equilibrium fictive temperature fluctuation $\sigma_{T_f^e}$ and independently evaluated thermodynamic quantities ΔC_p and S_c, we now test the quantitative validity of Eqs. 15&16 by comparing the predicted temperature dependence of the nonexponentiality parameter β_{KWW} with reported experimental values. Importantly, this comparison involves no adjustable fitting parameters.

Panel (a)–(c) in Fig. 4 show the equilibrium fictive temperature fluctuation $\sigma_{T_\mathrm{f}^\mathrm{e}}$ for B_2O_3, $Pd_{43}Cu_{27}Ni_{10}P_{20}$, and PVAc, respectively. The reported $\sigma_{T_\mathrm{f}^\mathrm{e}}$ for B_2O_3 are measured by DSC and modulated-DSC [46].

For $Pd_{43}Cu_{27}Ni_{10}P_{20}$, we use $\sigma_{T_\mathrm{f}^\mathrm{e}}$ reported in Ref. [47] measured by Flash-DSC. For PVAc, $\sigma_{T_\mathrm{f}^\mathrm{e}}$ is obtained from the reported glass transition temperature width ΔT_β measured by Flash-DSC in Ref. [48] using Schawe's vitrification function κ [31] as

$$\sigma_{T_\mathrm{f}^\mathrm{e}} = \frac{\Delta T_\beta}{2\kappa}. (23)$$

For $\sigma_{T_\mathrm{f}^\mathrm{e}}$, the independently reported values by Tombari *et al.* [40] and Hempel *et al.* [46] are used. This was done because we found the deviation of the reported $\sigma_{T_\mathrm{f}^\mathrm{e}}$ in Ref. [48] from the values measured by M-DSC.

Using these $\sigma_{T_\mathrm{f}^\mathrm{e}}$ values as inputs, Eqs. 15 and 16 yield predictions for β_KWW. The results are shown as red circles in Panels (d)–(f) of Fig. 4 and are compared with experimental β_KWW values obtained from various techniques such as dielectric spectroscopy, mechanical spectroscopy, and ultrasonic sound-velocity measurements compiled from the literature (see Fig. 4 caption for details and the values listed in the SM). Despite the distinct differences in chemistry, structure, and kinetics (fragility) among the three systems, the predicted β_KWW values show quantitative agreement with experiment across the accessible temperature range.

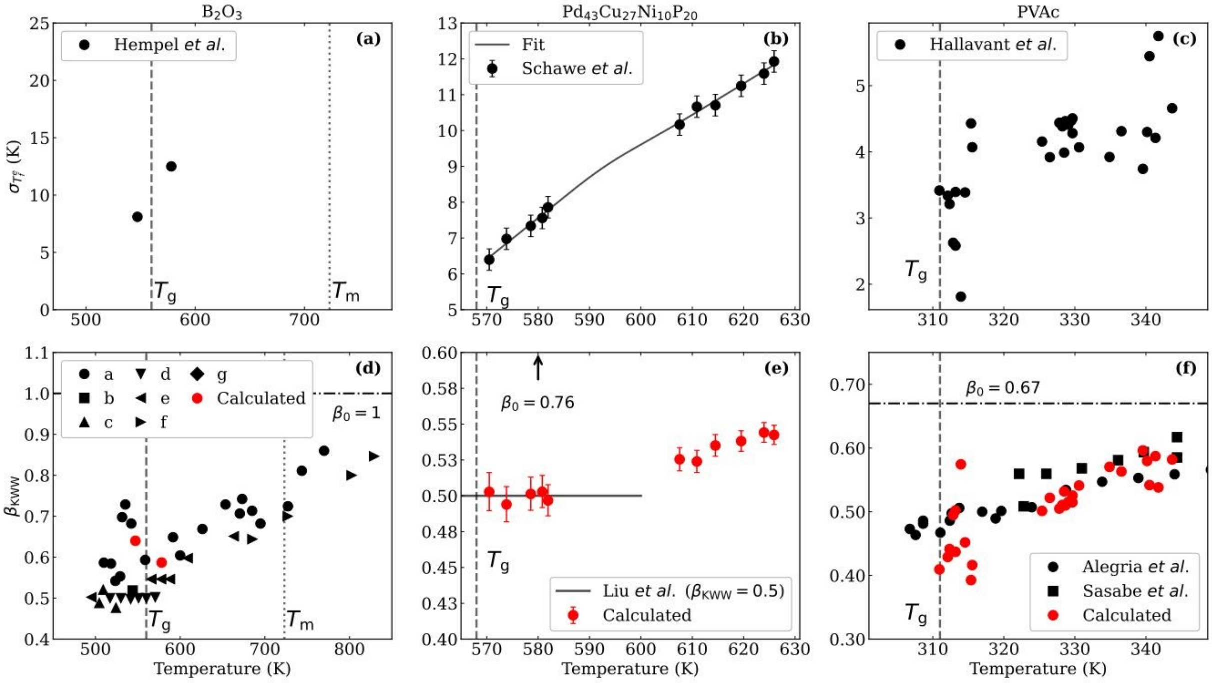

FIG 4. Equilibrium fictive-temperature fluctuations $\sigma_{T_\mathrm{f}^\mathrm{e}}$ in (a) B_2O_3, (b) $Pd_{43}Cu_{27}Ni_{10}P_{20}$, and (c) PVAc. $\sigma_{T_\mathrm{f}^\mathrm{e}}$ for B_2O_3 is taken from Ref.[46]; for $Pd_{43}Cu_{27}Ni_{10}P_{20}$, it is taken from Ref. [47]; for PVAc, it is calculated from the reported ΔT_β in Ref. [48] (see SM). The solid line in panel (b) shows the fit used to obtain smoothed $\sigma_{T_\mathrm{f}^\mathrm{e}}(T)$ data for calculating the fictive temperature fluctuation rate $R(T)$ in Eq. 19. Panels (d-f) show the corresponding β_KWW predicted from Eq. 15–16 (red circles) compared with experimental values (black markers). For B_2O_3 in (d), data labeled a is taken from Ref.[49] b–g from Ref. [50]. For $Pd_{43}Cu_{27}Ni_{10}$

View Article Online
DOI: 10.1039/D6MA00442C

P_{20} in (e), β_{KWW} values reported by Liu *et al.* [29] is shown as a solid line. For PVAc in (f), black circles are from Alegria *et al.* [37] and black squares from Sasabe *et al.* [51]

V. Time-Temperature Superposition

The assumption of time-temperature superposition (TTS) for analyzing relaxation dynamics in supercooled liquids and glasses works remarkably well near the standard T_g [17,18,52], where the relaxation time is on the order of 100 seconds. However, numerous studies have reported that this assumption breaks down at temperatures far from T_g [32,53,54], leading to what is commonly referred to as thermorheologically complex behavior.

The analysis developed in Section III.B suggests that the validity or breakdown of TTS is not simply a consequence of the temperature range considered, but instead reflects a balance between the fictive temperature fluctuation rate $R(T)$ and the configurational term $\Xi(T)$, as defined in Eq. 19 and Eq. 20, respectively. To validate these derived conditions, smoothed $\sigma_{T_f^e}(T)$ data for $Pd_{43}Cu_{27}Ni_{10}P_{20}$, obtained by fitting the two linear regimes with a sigmoid function (solid line in Fig. 4(c)), are used (see the SM for detailed method). This system is chosen because the available $\sigma_{T_f^e}$ data exhibit comparatively small experimental uncertainty.

As summarized in Table 1, when $R(T) - \Xi(T) = 0$, the system exhibits TTS, when $R(T) - \Xi(T) < 0$, β_{KWW} increases upon heating, and when $R(T) - \Xi(T) > 0$, β_{KWW} decreases upon heating, In Fig. 5, the difference between the calculated $R(T)$, evaluated using Eq. 19, and $\Xi(T)$ evaluated using Eq. 20 is plotted as a function of the predicted β_{KWW}. When $R(T) - \Xi(T) = 0$, the system exhibits TTS and when $R(T) - \Xi(T) < 0$, β_{KWW} increases upon heating in agreement with the predictions in Table 1 established from Eq 18-20. The horizontal error bars represent 95% confidence from the linear fits to $\sigma_{T_f^e}$ in Fig. 4(b), while the vertical error bars are from the experimental uncertainty in $\sigma_{T_f^e}$ shown in Fig.4(e). The figure shows that when β_{KWW} remains approximately constant near T_g, the quantity $R(T) - \Xi(T)$ approaches zero, thereby confirming the internal consistency of the present derivation.

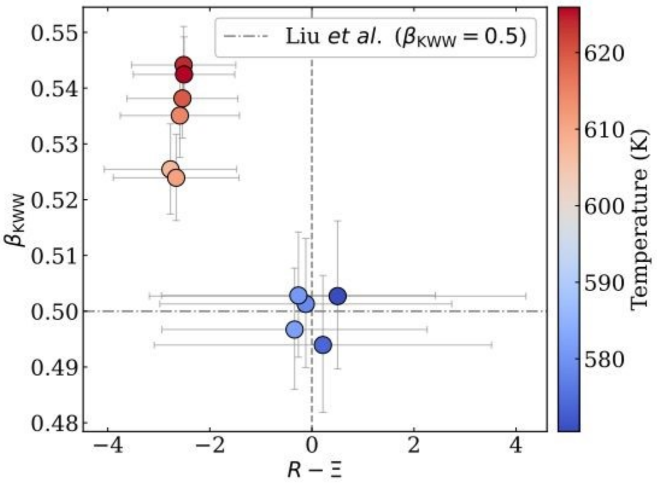

FIG 5. Difference $R(T) - \Xi(T)$ evaluated using Eqs. 19 and 20, plotted as a function of the predicted β_{KWW} for $Pd_{43}Cu_{27}Ni_{10}P_{20}$. Error bars represent 95% confidence intervals from linear fits' in Fig. 4(b), and the uncertainty in β_{KWW} arising from the experimental $\sigma_{T_f^e}(T)$. The color indicates temperature (see color bar). The dot-dashed line denotes the experimental

View Article Online
DOI: 10.1039/D6MA00442C

β_{KWW} near T_{g}, and the vertical dashed line indicates the TTS condition $R(T) = \Xi(T)$ summarized in Table 1.

VI. Discussion

The successful application of the proposed framework was demonstrated for three chemically, structurally, and kinetically distinct glass-forming systems. The agreement between predictions and measurements, obtained without any adjustable fitting parameters, demonstrates that the correlations between the nonexponentiality parameter β_{KWW} and the fictive temperature fluctuation $\sigma_{T_{\mathrm{f}}^{\mathrm{e}}}$, established in Eqs. 15&16 are physically consistent and applicable to a broad range of glass-forming systems.

The current approach does not rely on a particular functional form for $\Delta C_{\mathrm{p}}(T)$, $S_{\mathrm{c}}(T)$, β_{KWW}, and $\sigma_{T_{\mathrm{f}}^{\mathrm{e}}}$. Furthermore, extending the Adam–Gibbs equation to account for dynamic fluctuations (Eq. 11) through DFDT relation allows us to investigate not only the relationship between the configurational entropy $S_{\mathrm{c}}(T)$, and the average dynamics $\langle\tau\rangle$ as in the standard AG equation (Eq. 9), but also the fluctuations of the dynamic and thermodynamic quantities, $\sigma_{\ln\tau}$ and $\sigma_{T_{\mathrm{f}}^{\mathrm{e}}}$. Since the equilibrium fictive temperature is proportional to the enthalpy, $\sigma_{T_{\mathrm{f}}^{\mathrm{e}}}$ directly reflects the magnitude of local enthalpy fluctuations in the supercooled liquid. The framework thus provides a quantitative link between the enthalpy fluctuation and the nonexponential relaxation spectrum through the configurational entropy and heat capacity.

The model further yields a thermodynamic condition for time–temperature superposition (TTS), requiring a balance between the temperature dependence of $\sigma_{T_{\mathrm{f}}^{\mathrm{e}}}$, defined as the fictive temperature fluctuation rate $R(T)$, and the configurational term $\Xi(T)$. Wang and Richert [17] found that β_{KWW} remains constant from T_{g} up to a crossover temperature T_{c} (TTS regime), then rises steeply toward 1 at high T. They plot β_{KWW} against $\log_{10}\nu_{\max}$, the peak frequency of the α-relaxation loss spectrum at different temperature. The range of $\log_{10}\nu_{\max}$ over which β_{KWW} stays flat expands systematically with fragility m: strong liquids show no TTS at all, while fragile liquids maintain TTS from T_{g} all the way to T_{c}, covering up to ~8 decades. Above T_{c}, all systems converge to Debye relaxation ($\beta = 1$) by $\nu_{\max} \sim 10$GHz regardless of m. Similar behavior was observed in shear mechanical spectroscopy measurements of inorganic systems by Sen and Lovi [16]. In the current framework, the TTS condition (Eq. 18) is:

$$T\frac{d\ln\sigma_{T_{\mathrm{f}}^{\mathrm{e}}}(T)}{dT} = 2 + \frac{\Delta C_{\mathrm{p}}(T)}{S_{\mathrm{c}}(T)} - T\frac{d}{dT}\ln\left(1 + \frac{\Delta C_{\mathrm{p}}(T)}{S_{\mathrm{c}}(T)}\right).$$

It has been previously established that $\Delta C_{\mathrm{p}}(T)/S_{\mathrm{c}}(T)$ and the rate of change of $S_{\mathrm{c}}(T)$ are directly correlated to fragility [12,13]. Indeed, for the three systems investigated, both the ratio $\Delta C_{\mathrm{p}}(T)/S_{\mathrm{c}}(T)$ and the magnitude of its slope are larger for more fragile systems, as shown in Fig. 3(b). This implies that the right-hand side of Eq. 18 (shown above) will be larger for more fragile systems. Consequently, for TTS to hold, the rate at which the equilibrium fictive temperature fluctuation increase must also be larger. The empirical observation that fragile systems maintain TTS over a wider range of relaxation times thus indicates that the temperature dependence of the fictive temperature fluctuation is stronger in fragile systems. However, the fictive temperature fluctuation rate is itself temperature-dependent, as seen in the analysis of $\mathrm{Pd_{43}Cu_{27}Ni_{10}P_{20}}$ in Fig. 5 supporting the eventual

View Article Online
DOI: 10.1039/D6MA00442C

breakdown of TTS even for fragile liquids at high temperature, as observed by Wang and Richert [17].

VII. Conclusion

This work developed a framework that connects thermodynamic fluctuations and dynamic heterogeneity in supercooled liquids by extending the Adam–Gibbs relation through DFDT formalism. This approach establishes a direct relation between the equilibrium fictive-temperature fluctuation $\sigma_{T_\mathrm{f}^\mathrm{e}}$, which reflects the underlying distribution of local enthalpies, and the nonexponential parameter β_KWW through thermodynamic quantities: the configurational entropy $S_\mathrm{c}(T)$ and the heat capacity difference between glass and liquid ΔC_p (T). The successful application of the framework was demonstrated for three chemically, structurally, and kinetically distinct glass-forming systems. The agreement between predictions and measurements, obtained without any adjustable fitting parameters, indicates that the derived expression in Eq. 15 is physically consistent and applicable to a broad range of glass-forming systems. The model further yields a thermodynamic condition for time–temperature superposition (TTS), which requires a balance between the temperature dependence of $\sigma_{T_\mathrm{f}^\mathrm{e}}$, defined as the fictive temperature fluctuation rate $R(T)$, and the configurational term $\Xi(T)$, related to $S_\mathrm{c}(T)$, and $\Delta C_\mathrm{p}(T)$, and their temperature dependence. These results provide a thermodynamic connection to dynamic heterogeneity and TTS in supercooled liquids. Further validation would require a more integrated examination of the relationships among the temperature dependence of fictive temperature fluctuations (enthalpy fluctuation), configurational entropy, and dynamic heterogeneity in glass-forming systems. Future work combining experiments and atomistic simulations may further clarify the structural origins of these relationships.

Acknowledgments:

The authors acknowledge financial support from NSF-DMR under grant#: 1832817.

References:

[1] M.D. Ediger, Spatially Heterogeneous Dynamics in Supercooled Liquids, Annu. Rev. Phys. Chem. 51 (2000) 99–128. https://doi.org/10.1146/annurev.physchem.51.1.99.

[2] P.G. Debenedetti, F.H. Stillinger, Supercooled liquids and the glass transition, Nature 410 (2001) 259–267. https://doi.org/10.1038/35065704.

[3] R. Richert, Heterogeneous dynamics in liquids: fluctuations in space and time, Journal of Physics: Condensed Matter 14 (2002) R703. https://doi.org/10.1088/0953-8984/14/23/201.

[4] R. Kohlrausch, Theorie des elektrischen Rückstandes in der Leidener Flasche, Annalen Der Physik Und Chemie 167 (1854) 179–214. https://doi.org/10.1002/andp.18541670103.

[5] G. Williams, D.C. Watts, Non-symmetrical dielectric relaxation behaviour arising from a simple empirical decay function, Transactions of the Faraday Society 66 (1970) 80–85. https://doi.org/10.1039/TF9706600080.

View Article Online
DOI: 10.1039/D6MA00442C

[6] R. Richert, Homogeneous dispersion of dielectric responses in a simple glass, J. Non. Cryst. Solids 172–174 (1994) 209–213. https://doi.org/10.1016/0022-3093(94)90436-7.

[7] K.L. Ngai, Temperature dependence of the stretched exponent in structural relaxation of fragile glass-forming molecular liquids, J. Non. Cryst. Solids 131–133 (1991) 80–83. https://doi.org/10.1016/0022-3093(91)90277-D.

[8] K.L. Ngai, S.W. Martin, Correlatioin between the activation enthalpy and Kohlrausch exponent for ionic conductivity in oxide glasses, Phys. Rev. B 40 (1989).

[9] P. Zhang, J.J. Maldonis, Z. Liu, J. Schroers, P.M. Voyles, Spatially heterogeneous dynamics in a metallic glass forming liquid imaged by electron correlation microscopy, Nat. Commun. 9 (2018).

[10] P.K. Dixon, S.R. Nagel, Frequency-Dependent Specific Heat and Thermal Conductivity at the Glass Transition in o-Terphenyl Mixtures, Phys. Rev. Lett. 61 (1988) 341–344. https://doi.org/10.1103/PhysRevLett.61.341.

[11] C.A. Angell, Relaxation in liquids, polymers and plastic crystals — strong/fragile patterns and problems, J. Non. Cryst. Solids 131–133 (1991) 13–31. https://doi.org/10.1016/0022-3093(91)90266-9.

[12] L.M. Martinez, C.A. Angell, A thermodynamic connection to the fragility of glass-forming liquids, Nature 410 (2001) 663–667. https://doi.org/10.1038/35070517.

[13] L.M. Wang, C.A. Angell, R. Richert, Fragility and thermodynamics in nonpolymeric glass-forming liquids, Journal of Chemical Physics 125 (2006). https://doi.org/10.1063/1.2244551.

[14] V. Lubchenko, P.G. Wolynes, Theory of aging in structural glasses, Journal of Chemical Physics 121 (2004) 2852–2865. https://doi.org/10.1063/1.1771633.

[15] R. Böhmer, K.L. Ngai, C.A. Angell, D.J. Plazek, Nonexponential relaxations in strong and fragile glass formers, J. Chem. Phys. 99 (1993) 4201–4209. https://doi.org/10.1063/1.466117.

[16] S. Sen, J. Lovi, Trends in the temperature dependence of dynamical heterogeneity in strong and fragile supercooled liquids, J. Non. Cryst. Solids 638 (2024) 123060. https://doi.org/10.1016/j.jnoncrysol.2024.123060.

[17] L.M. Wang, R. Richert, Primary and secondary relaxation time dispersions in fragile supercooled liquids, Phys. Rev. B Condens. Matter Mater. Phys. 76 (2007) 1–8. https://doi.org/10.1103/PhysRevB.76.064201.

[18] N.B. Olsen, T. Christensen, J.C. Dyre, Time-temperature superposition in viscous liquids, Phys. Rev. Lett. 86 (2001) 1271–1274. https://doi.org/10.1103/PhysRevLett.86.1271.

[19] E. Donth, General derivation of the WLF equation from a fluctuation approach to the glass transition, Acta Polymerica 30 (1979) 481–485. https://doi.org/https://doi.org/10.1002/actp.1979.010300804.

View Article Online
DOI: 10.1039/D6MA00442C

[20] E.W. Fischer, E. Donth, W. Steffen, Temperature dependence of characteristic length for glass transition, Phys. Rev. Lett. 68 (1992) 2344–2346. https://doi.org/10.1103/PhysRevLett.68.2344.

[21] J.C. Mauro, R.J. Loucks, Selenium glass transition: A model based on the enthalpy landscape approach and nonequilibrium statistical mechanics, Phys. Rev. B Condens. Matter Mater. Phys. 76 (2007) 174202. https://doi.org/10.1103/PhysRevB.76.174202.

[22] J.C. Mauro, R.J. Loucks, J. Balakrishnan, S. Raghavan, Monte Carlo method for computing density of states and quench probability of potential energy and enthalpy landscapes, Journal of Chemical Physics 126 (2007). https://doi.org/10.1063/1.2733674.

[23] C.T. Moynihan, J. Schroeder, Non-exponential structural relaxation, anomalous light scattering and nanoscale inhomogeneities in glass-forming liquids, J. Non. Cryst. Solids 160 (1993) 52–59. https://doi.org/10.1016/0022-3093(93)90283-4.

[24] J. Schroeder, M. Lee, S.K. Saha, J.H. Whang, C.T. Moynihan, Independently relaxing nanoscale inhomogeneities as a model for structural relaxation: Light scattering around the glass transition region, J. Non. Cryst. Solids 203 (1996) 186–191. https://doi.org/10.1016/0022-3093(96)00500-5.

[25] M. Lee, S.K. Saha, C.T. Moynihan, J. Schroeder, Non-exponential structural relaxation, anomalous light scattering and nanoscale inhomogeneities in glasses, J. Non. Cryst. Solids 222 (1997) 369–375. https://doi.org/10.1016/S0022-3093(97)90138-1.

[26] W. Takeda, P. Lucas, A model of heterogeneous undercooled liquid and glass accounting for temperature-dependent nonexponentiality and enthalpy fluctuation, J. Chem. Phys. 160 (2024) 174504. https://doi.org/10.1063/5.0196812.

[27] G. Adam, J.H. Gibbs, On the Temperature Dependence of Cooperative Relaxation Properties in Glass-Forming Liquids, J. Chem. Phys. 43 (1965) 139–146. https://doi.org/https://doi.org/10.1063/1.1696442.

[28] K.J. Crowley, G. Zografi, The use of thermal methods for predicting glass-former fragility, Thermochim. Acta 380 (2001) 79–93. https://doi.org/10.1016/S0040-6031(01)00662-1.

[29] C. Liu, E. Pineda, J. Qiao, D. Crespo, Modeling of the Sub-Tg Relaxation Spectrum of Pd42.5Ni7.5Cu30P20 Metallic Glass, Journal of Physical Chemistry B 120 (2016) 2838–2844. https://doi.org/10.1021/acs.jpcb.5b11754.

[30] E. Donth, Characteristic length of the glass transition, J. Polym. Sci. B Polym. Phys. 34 (1996) 2881–2892. https://doi.org/10.1002/(SICI)1099-0488(199612)34:17<2881::AID-POLB3>3.0.CO;2-U.

[31] J.E.K. Schawe, Vitrification in a wide cooling rate range: The relations between cooling rate, relaxation time, transition width, and fragility, Journal of Chemical Physics 141 (2014) 184905. https://doi.org/10.1063/1.4900961.

[32] D. Cangialosi, A. Alegría, J. Colmenero, On the temperature dependence of the nonexponentiality in glass-forming liquids, J. Chem. Phys. 130 (2009) 124902. https://doi.org/10.1063/1.3098904.

[33] I.M. Hodge, Adam-Gibbs Formulation of Nonlinearity in Glassy-State Relaxations, Macromolecules 19 (1986) 936–938. https://doi.org/10.1021/ma00157a082.

[34] I. Gallino, J. Schroers, R. Busch, Kinetic and thermodynamic studies of the fragility of bulk metallic glass forming liquids, J. Appl. Phys. 108 (2010). https://doi.org/10.1063/1.3480805.

[35] P.K. Gupta, J.C. Mauro, Two factors governing fragility: Stretching exponent and configurational entropy, Phys. Rev. E Stat. Nonlin. Soft Matter Phys. 78 (2008) 1–3. https://doi.org/10.1103/PhysRevE.78.062501.

[36] R. Richert, M. Richert, Dynamic heterogeneity, spatially distributed stretched-exponential patterns, and transient dispersions in solvation dynamics, Phys. Rev. E Stat. Phys. Plasmas Fluids Relat. Interdiscip. Topics 58 (1998) 779–784. https://doi.org/10.1103/PhysRevE.58.779.

[37] A. Alegría, J. Colmenero, P.O. Mari, I.A. Campbell, Dielectric investigation of the temperature dependence of the nonexponentiality of the dynamics of polymer melts, Phys. Rev. E Stat. Phys. Plasmas Fluids Relat. Interdiscip. Topics 59 (1999) 6888–6895. https://doi.org/10.1103/PhysRevE.59.6888.

[38] B.Y.J.C. Southard, The Thermal Properties of Crystalline and Glassy Boron Trioxide, Journal of the American Ceramic Society 63 (1941) 3147–3150. https://doi.org/10.1021/ja01856a073.

[39] A. Meyer, R. Busch, H. Schober, Time-temperature superposition of structural relaxation in a viscous metallic liquid, Phys. Rev. Lett. 83 (1999) 5027–5029. https://doi.org/10.1103/PhysRevLett.83.5027.

[40] E. Tombari, C. Ziparo, G. Salvetti, G.P. Johari, Vibrational and configurational heat capacity of poly(vinyl acetate) from dynamic measurements, Journal of Chemical Physics 127 (2007). https://doi.org/10.1063/1.2747596.

[41] H.L. Smith, C.W. Li, A. Hoff, G.R. Garrett, D.S. Kim, F.C. Yang, M.S. Lucas, T. Swan-Wood, J.Y.Y. Lin, M.B. Stone, D.L. Abernathy, M.D. Demetriou, B. Fultz, Separating the configurational and vibrational entropy contributions in metallic glasses, Nat. Phys. 13 (2017) 900–905. https://doi.org/10.1038/nphys4142.

[42] S.B. Thomas, G.S. Parks, Studies on Glass. VI. Some Specific Heat Data on Boron Trioxide, J. Phys. Chem. 35 (1931) 2091–2102. https://doi.org/10.1021/j150325a016.

[43] M. Kuno, L.A. Shadowspeaker, J. Schroers, R. Busch, Thermodynamics of the Pd43Ni10Cu27P 20bulk metallic glass forming alloy, Materials Research Society Symposium - Proceedings 806 (2003) 227–232. https://doi.org/10.1557/proc-806-mm5.2.

View Article Online
DOI: 10.1039/D6MA00442C

[44] U. Gaur, B.B. Wunderlich, B. Wunderlich, Heat Capacity and Other Thermodynamic Properties of Linear Macromolecules. VII. Other Carbon Backbone Polymers, J. Phys. Chem. Ref. Data 12 (1983) 29–63. https://doi.org/10.1063/1.555677.

[45] J.Y. Tsao, Two semiempirical expressions for condensed-phase heat capacities, J. Appl. Phys. 68 (1990) 1928–1930. https://doi.org/10.1063/1.346588.

[46] E. Hempel, G. Hempel, A. Hensel, C. Schick, E. Donth, Characteristic Length of Dynamic Glass Transition near Tg for a Wide Assortment of Glass-Forming Substances, Journal of Physical Chemistry B 104 (2000) 2460–2466. https://doi.org/10.1021/jp991153f.

[47] J.E.K. Schawe, M.K. Kwak, M. Stoica, E.S. Park, J.F. Löffler, The Cooperativity of Atomic Fluctuations in Highly Supercooled Glass-Forming Metallic Melts, Journal of Physical Chemistry Letters 16 (2025) 948–954. https://doi.org/10.1021/acs.jpclett.4c03275.

[48] K. Hallavant, M. Mejres, J.E.K. Schawe, A. Esposito, A. Saiter-Fourcin, Influence of Chemical Composition and Structure on the Cooperative Fluctuation in Supercooled Glass-Forming Liquids, Journal of Physical Chemistry Letters 15 (2024) 4508–4514. https://doi.org/10.1021/acs.jpclett.4c00632.

[49] D. Sidebottom, R. Bergman, L. Börjesson, L.M. Torell, Two-step relaxation decay in a strong glass former, Phys. Rev. Lett. 71 (1993) 2260–2263. https://doi.org/10.1103/PhysRevLett.71.2260.

[50] G.M. Bartenev, V.A. Lomovskoi, Relaxation time spectra and the peculiarities of the process of boron anhydride glass transition, J. Non. Cryst. Solids 146 (1992) 225–232. https://doi.org/10.1016/S0022-3093(05)80495-8.

[51] H. Sasabe, C.T. Moynihan, Structural Relaxation in Poly(Vinyl Acetate)., J Polym Sci Polym Phys Ed 16 (1978) 1447–1457. https://doi.org/10.1002/pol.1978.180160810.

[52] J. Zhao, G.B. McKenna, Temperature divergence of the dynamics of a poly(vinyl acetate) glass: Dielectric vs. mechanical behaviors, Journal of Chemical Physics 136 (2012) 154901. https://doi.org/10.1063/1.3701736.

[53] G.W. Scherer, Volume Relaxation Far from Equilibrium, Journal of the American Ceramic Society 69 (1986) 374–381. https://doi.org/10.1111/j.1151-2916.1986.tb04764.x.

[54] R.F. Lancelotti, E.D. Zanotto, S. Sen, Kinetics of physical aging of a silicate glass following temperature up- and down-jumps, J. Chem. Phys. 160 (2024) 034504. https://doi.org/10.1063/5.0185538.

View Article Online
DOI: 10.1039/D6MA00442C

Data Availability

This study does not report any new experimental data. The data reported in this study are modeled from experimental data available in the cited literature. All modeled data are included in the manuscript and the supplemental material.